Ascorbate degradation in tomato leads to accumulation of oxalate, threonate and oxalyl threonate

Citation for published version:
Truffault, V, Fry, S, Stevens, RG & Gautier, H 2016, 'Ascorbate degradation in tomato leads to accumulation of oxalate, threonate and oxalyl threonate: Ascorbate degradation in tomato', *The Plant Journal*. https://doi.org/10.1111/tpj.13439

Digital Object Identifier (DOI):
10.1111/tpj.13439

Published In:
The Plant Journal

ASCORBATE DEGRADATION IN TOMATO LEADS TO ACCUMULATION OF OXALATE, THREONATE AND OXALYL THREONATE

Vincent Truffault[1, 2], Stephen C. Fry[3], Rebecca G. Stevens[1] and Hélène Gautier[2]

[1] *INRA, UR-1052, Génétique et Amélioration des Fruits et Légumes, Domaine St Maurice, 84143 Montfavet, France*

[2] *INRA, UR-1115, Plantes et Systèmes de culture Horticoles, centre PACA, Domaine Saint Paul, 84914 Avignon Cedex, France*

[3] *The Edinburgh Cell Wall Group, Institute of Molecular Plant Sciences, School of Biological Sciences, The University of Edinburgh, Daniel Rutherford Building, The King's Building, Edinburgh EH9 3BF, UK*

Running title: Ascorbate degradation in tomato

Significance statement: Ascorbate is a key molecule for plant metabolism and a marker of fruit nutritional quality, but how it is degraded is poorly studied *in vivo*. Here we used radiolabeling to determine which degradation products accumulate in tomato leaves, to evaluate how the ascorbate pool size affects the degradation rate, and to test whether the degradation rate could be reduced by manipulating an enzyme involved in ascorbate recycling. We suggest that controlling ascorbate degradation might be a means to increase or stabilize ascorbate content.

Word count: 6540 words

Abstract: Ascorbate content in plants is controlled by its synthesis from carbohydrates, recycling of the oxidized forms and degradation. Of these pathways, ascorbate degradation is the least studied and represents a lack of knowledge which could impair improvement of ascorbate content in fruits and vegetables as degradation is non-reversible and leads to a depletion of the ascorbate pool. The present study revealed the nature of degradation products using [^{14}C]ascorbate labelling in tomato, a model plant for fleshy fruits; oxalate and threonate are accumulated in leaves, as is oxalyl threonate. Carboxypentonates coming from diketogulonate degradation were detected in relatively insoluble (cell wall-rich) leaf material. No [^{14}C]tartaric acid was found in tomato leaves. Ascorbate degradation was stimulated by darkness, and the degradation rate was evaluated at 63% of the ascorbate pool per day, a percentage that was constant and independent of the initial ascorbate or dehydroascorbic acid concentration over periods of 24h or more. Furthermore, degradation could be partially affected by the ascorbate recycling pathway, as lines under-expressing monodehydroascorbate reductase showed a slight decrease in degradation product accumulation.

Keywords: ascorbate degradation, monodehydroascorbate reductase, light environment, tomato, [^{14}C]ascorbate labelling, high voltage paper electrophoresis.

L-Ascorbate (AsA) is a small organic acid derived from sugars. In plants, ascorbate is a key molecule involved in numerous cellular processes (cell division and expansion, photo-protection, enzyme cofactor, cell signalling; Smirnoff and Wheeler, 2000). Ascorbate is an essential antioxidant for plants, protecting the cell from reactive oxygen species (ROS). Curiously, ascorbate can also serve as a pro-oxidant, generating for example the highly reactive hydroxyl radical ($^{\bullet}OH$; Fry, 1998). The cellular concentration of ascorbate depends on its transport, biosynthesis, recycling and degradation: these are under genetic control and closely related to environmental conditions. According to multiple studies, one of the key genes of the biosynthetic pathway is *vtc2* (coding for GDP-L-galactose phosphorylase) which is up-regulated by light in leaves (Laing et al., 2015). Recycling of ascorbate's oxidation products (MDHA or dehydroascorbic acid (DHA)) to the reduced form (AsA) occurs via two enzymes monodehydroascorbate reductase (MDHAR) and DHA reductase (DHAR). MDHAR is an NAD(P)H-dependent enzyme which can reduce MDHA to AsA. DHAR uses glutathione as electron donor to reduce DHA to AsA. If not reduced by MDHAR or DHAR, MDHA and DHA may be further degraded, resulting in irreversible loss of ascorbate.

Ascorbate degradation in mammals, as in plants, has been poorly studied. In Figure 1, we sum up current knowledge about ascorbate degradation in mammals (vii and viii) and plants (i to vi). Degradation occurs *in vitro* via the unstable oxidized form DHA and can lead to the accumulation of end-products 2,3-diketo-L-gulonate, L-erythrulose (Nemet and Monnier, 2011), oxalate, L-threonate, L-xylosone (xylosulose), L-lyxonate, L-threosone and 3-deoxythreosone (Simpson and Ortwerth, 2000; Linster and Van Schaftingen, 2007). In humans, ascorbate degradation has been followed using radiolabelling experiments. After ingestion in the human body, 44% of the radioactivity from [1-^{14}C]ascorbate could be recovered in urine as oxalate, 20% as diketogulonate and 2% as DHA (Hellman and Burns, 1958). Recently, multiple studies have shown that ascorbate degradation products could interact with proteins and lead to the formation of advanced-glycation-end-products (AGE), suspected to play a role in complications in diabetes and cellular degeneration (Regulus et al., 2010; Kay et al., 2013). In *Escherichia coli* (Figure 1 ix), ascorbate can be used as source of carbon under anaerobic conditions, through enzymatic degradation to generate D-xylulose 5-phosphate, which can then participate in the pentose phosphate pathway (Yew and Gerlt, 2002).

In plants, the *in vivo* degradation pathway involves enzymatic reactions as well as non-enzymatic ones starting from ascorbate or DHA (Green and Fry, 2005a). End-products of the degradation pathway are species-dependent and include L-tartrate or oxalate and L-threonate (Figure 1; Green & Fry 2005b; Hancock & Viola 2005; DeBolt *et al.* 2006; Melino *et al.* 2009). Tartrate is mainly formed by cleavage of the ascorbate skeleton between carbons 4 and 5; in this pathway, the tartrate would thus be derived from carbons 1–4 of the ascorbate. The only

enzyme in this pathway identified for the moment is L-idonate dehydrogenase (DeBolt et al., 2006), which catalyzes the conversion of L-idonate (derived from ascorbate) into 5-keto-gluconic acid, a precursor of L-tartrate. This degradation pathway may occur enzymatically or non-enzymatically in species such as grape (grape berries are also known to accumulate oxalate (DeBolt et al., 2004), and thus use two degradation pathways within the same organ) and other *Vitaceae* (Hancock and Viola, 2005). Tartrate accumulation could also be the result of a conversion of L-threonate to L-tartrate, as in *Pelargonium crispum* (Wagner and Loewus, 1973), in which case the tartrate would be derived from carbons 3–6 of the ascorbate. In grape berries, tartaric acid deriving from ascorbate degradation is stored as calcium or potassium salts (DeBolt et al., 2004) during fruit development until 50 days after anthesis, but it appears that only a small proportion of the total ascorbate is actually used for the synthesis of L-tartrate (Melino et al., 2009). Tartaric acid is the major acid found in wine, contributing to its taste.

The formation of oxalate and threonate results from the cleavage of DHA between carbons 2 and 3. Intermediates between DHA and the oxalate and threonate end-products in the apoplast of *Rosa* cells (Green and Fry, 2005b) were initially proposed to be, sequentially, cyclic oxalyl L-threonates and oxalyl L-threonates. However, a kinetic study clarified that cyclic oxalyl L-threonates, oxalyl L-threonates and oxalate + threonate are all formed simultaneously, presumably from a highly reactive initial oxidation product of DHA, proposed to be cyclic-2,3-*O*-oxalyl-L-threonolactone (Parsons et al., 2011). This branched degradation pathway, observed in the apoplast and *in vitro*, might also occur in other cellular compartments. The proposed pathway could occur non-enzymatically *in vitro* but some steps are catalyzed by unknown enzymes as some reactions occur more rapidly *in vivo* (Green and Fry, 2005b). In lemon geranium, L-threonate is accumulated (Helsper and Loewus, 1982) but can also be decarboxylated to L-glycerate (Loewus, 1999). Oxalate accumulates in spinach, wood sorrel, shamrock and begonia (Yang and Loewus, 1975). In dock leaves (Helsper and Loewus, 1982), 24h radiolabelling experiments with [U-^{14}C]ascorbate revealed the following radioactive distribution: 1% in tartaric acid, 14% in threonic acid, 11% in oxalic acid, 14% in remaining ascorbate, 49% in others compounds and 11% in carbon dioxide (CO_2). When oxidation is minimised, DHA degradation occurs instead via hydrolysis into diketogulonate (DKG degradation branch; Fig. 1). Diketogulonate can be rearranged to form lactones provisionally identified as carboxypentonates, which can themselves be de-lactonised but are otherwise stable *in vivo* (Parsons et al., 2011); DKG can itself also be oxidised (Parsons and Fry, 2012).

There is little information about the potential role of these degradation products in plant cells. Oxalate is a very simple dicarboxylate which can be found in vacuoles (as also its soluble potassium, sodium or magnesium salts or insoluble calcium salts). Oxalate can be very abundant in oxalate-accumulating plants, reaching 3% up to 38% of dry mass (Libert and

109 Franceschi, 1987). Oxalate can be rapidly linked to calcium leading to the formation of calcium
110 oxalate crystals, localized in vacuoles, cell walls (Khan, 1995) and specialized cells
111 (idioblasts). Ascorbate degradation could be the first source of oxalate required for the
112 formation of crystals with calcium in many species (Loewus, 1999; Franceschi and Nakata,
113 2005), with the exception of rice (Yu et al., 2010) and probably a few others species. Calcium
114 oxalate crystals are found in a wide diversity of plants and animals. These crystals may be
115 responsible for the regulation of the calcium pool of the cell (Nakata, 2003) but could also act
116 in the defence process against herbivory (Franceschi and Nakata, 2005). Oxalate can be
117 further oxidized in by oxalate oxidase (mostly reported in monocots) releasing H_2O_2 and CO_2
118 which may be used as an internal source for photosynthesis as oxalate oxidase is up-regulated
119 by light (Loewus, 1999, Tooulakou et al., 2016). In species with no oxalate oxidase activity like
120 in *Arabidopsis*, a cytoplasmic oxalyl-CoA synthetase may be required as a first step for oxalate
121 degradation to CO_2 (and formic acid; Foster et al., 2012), as also previously described in pea,
122 pumpkin and lupin seeds and wheat germ (Giovanelli, 1966).

123 Even if calcium oxalate crystal formation confers tissue rigidity and support, it has been
124 revealed that calcium oxalate crystals are not necessary for growth processes in *Medicago*
125 *truncatula* (Nakata and McConn, 2003; Nakata, 2012). Despite the remaining gaps in our
126 knowledge of ascorbate catabolism pathways, the degradation rate and the expression of
127 ascorbate oxidase are often positively correlated to cell expansion (Lin and Varner, 1991;
128 Dumville and Fry, 2003; Müller et al., 2009), which is curious since ascorbate oxidase degrades
129 ascorbate even though rapid growth usually correlates with high ascorbate concentrations.

130 Genetic and environmental impacts on ascorbate synthesis and recycling pathways
131 have been well studied in a large diversity of plants (Hamner et al., 1945; Bartoli et al., 2006;
132 Dowdle et al., 2007; Gautier et al., 2008; Massot et al., 2013). Light is proposed to be the most
133 important environmental parameter altering ascorbate content. Ascorbate biosynthesis is
134 activated by light: an increase of 66% in the ascorbate content in tomato leaves was found
135 when plants were transferred from darkness to light (Hamner et al., 1945), although it was
136 unclear whether this effect was due to increased biosynthesis or decreased degradation.
137 Environmental control of the degradation rate has been poorly studied. Conklin et al. (1997)
138 showed that radiolabelled ascorbate infiltrated into detached *Arabidopsis* leaves was rapidly
139 oxidized in 24h in the dark. In contrast, in leaves of wood sorrel, degradation occurred at the
140 same rate in light or darkness (Yang and Loewus, 1975).

141 *Solanum lycopersicum* is a model plant and one of the largest crops in the world. No
142 information on either degradation products or the degradation rate is available in tomato. In
143 this study, the aims were (i) to determine which degradation products accumulate in tomato

144 leaves; (ii) to evaluate the impact of ascorbate pool size on its degradation rate; (iii) to assay
145 potential adjustment of the degradation rate by the activity of ascorbate recycling (by
146 manipulation of MDHAR activity in transgenic plants). This study therefore aims to characterize
147 ascorbate degradation products and the degradation rate under the influence of both
148 environmental and genetic factors in tomato.

149 Materials and methods

150 Plant material and growth conditions:

151 *Solanum lycopersicum* L. variety West Virginia 106 (cherry tomato) cotyledons were
152 transformed as previously described by (Gest et al., 2013). Plantlets overexpressing MDHAR
153 were labelled sx lines in this paper. Plantlets underexpressing MDHAR were labelled mds lines
154 in this paper. Wild type plantlets were used as reference (WT). Tomato plantlets used for
155 radiolabelling experiments were grown in a greenhouse located at the University of Edinburgh,
156 Scotland. Tomato plantlets used for GC-MS analysis were grown in climatic chambers located
157 at INRA, Avignon. Tomato plantlets were acclimated for 2 weeks under short days (i.e. 8h
158 light/16h dark) in low light conditions (100 $\mu mol.m^{-2}.s^{-1}$) and then a batch of plantlets was placed
159 in high light conditions (1000 $\mu mol.m^{-2}.s^{-1}$) for 7 days while another batch stayed in low light for
160 7 days. A period of darkness for 48h was applied before final sampling to evaluate the effect
161 of ascorbate pool size on ascorbate degradation rate.

162 Chemicals:

163 Solid L-[1-^{14}C]ascorbic acid (0.52 or 0.407 $MBq.\mu mol^{-1}$) from GE Healthcare was dissolved in
164 water, aliquoted and stored at -80°C until required. [^{14}C]Mannitol (2.18 $MBq.\mu mol^{-1}$) was from
165 Amersham International.

166 Incubation of tomato leaves with [^{14}C]ascorbate:

167 Tomato leaves were picked at 9am and quickly transferred such that the cut base of the petiole
168 was in 5 kBq of [^{14}C]ascorbate diluted in 20µl of water. Pulse–chase incubation was performed.
169 A constant air circulation was maintained during the whole incubation, and after approximately
170 1h (when the detached leaves had totally absorbed the radioactive solution), the [^{14}C]ascorbate
171 solution was replaced by water. We followed radioactive ascorbate metabolism in a single
172 leaflet kept under darkness for 24h and 48h. Sampling was performed as per the following time
173 course: after 1 min of incubation, 30min, 1h, [add water], 2h, 3h, 4h, 6h, 8h and 24h. Tomato
174 leaflets were immediately stored at -80°C before grinding.

175 Extraction of [^{14}C]ascorbate derivatives:

176 Tomato lamina samples were first weighed (50-60mg per leaflet) and then ground to a powder
177 in liquid nitrogen. The powder was homogenized in 150µl of a solution containing 15% formic
178 acid to extract ascorbate derivatives and 1.25% of non-radioactive ascorbate to prevent from
179 further oxidation (the extraction process is summarized in Figure 2). One portion (10µl) of acid
180 supernatant was analyzed by high-voltage paper electrophoresis (HVPE), and a further portion
181 was assayed for total extracted radioactivity by scintillation counting. After quick rinses with
182 15% formic acid and water, the pellet was then treated with 2 ml of 1M sodium hydroxide
183 (NaOH) at room temperature for 30 min to extract an additional fraction (including any polymer-
184 linked esters). Half of the NaOH extract was scintillation counted, and half was dialysed against
185 distilled water (2 x 12h) in Thermo Scientific dialysis tubes (mol. wt. cut-off 12,000) to remove
186 small molecules while trapping polymers. After quick rinses with 1M NaOH and water, the
187 tomato leaf residue was treated with 2M trifluoroacetic acid (TFA) at room temperature for
188 15min and centrifuged, then the TFA supernatant was volatilized to dryness using a SpeedVac,
189 and extracts (10µl) were analyzed by HVPE. Radioactivity from all extracts was quantified by
190 scintillation counting.

191 **High-voltage paper electrophoresis (HVPE):**

192 HVPE is particularly valuable for kinetic analyses of unstable radiolabelled organic acids such
193 as ascorbate (Fry, 2011). Samples were dried on Whatman No.3 paper and electrophoresed
194 in a volatile buffer at pH6.5 (acetic acid-pyridine-water, 1:33:300 by volume, containing 5mM
195 EDTA) for 30min at 3.0kV or at pH2.0 (formic acid-acetic acid-water, 1:35:355 by volume) for
196 1h at 3.0kV. The papers were cooled to 20-25°C with toluene (for the pH6.5 buffer) or white
197 spirit (for pH2.0) during the run. A trace of Orange G was loaded with the samples and used
198 as an internal reference marker. Electrophoretic mobilities were reported as m_{OG} values
199 (mobility, corrected for electro-endo-osmosis, relative to that of orange G). Authentic markers
200 were purchased from Sigma Chemicals (Sigma) except for 2,3-diketogulonate, compound C
201 and compound E which were eluted from previous experiments (isolated by elution from
202 electrophoretograms in water). Non-radioactive compounds were stained with $AgNO_3$ or
203 bromophenol blue (Fry, 2011).

204 **Detection of radioactivity:**

205 ^{14}C-Labelled compounds on paper electrophoretograms were detected by autoradiography on
206 Kodak BioMax MR-1 film. Alternatively, paper electrophoretograms were cut into strips and
207 transferred into 23-ml Packard vials containing 2ml of Gold Star scintillant. Radioactive
208 solutions were mixed with 10 volumes of 'OptiScint HighSafe'. ^{14}C was quantified by
209 scintillation counting (LS 6500 Beckman; Beckman Coulter Ltd, High Wycombe, UK).

210 **Ascorbate content:**

211 Measurements of ascorbic acid content were carried out as previously described (Stevens et
212 al., 2006). Ground powder was stored at -80°C then extracted in ice-cold 6% trichloroacetic
213 acid (TCA). The spectrophotometric assay was based on the detection of dipyridyl-Fe^{2+}
214 complexes following the reduction of Fe^{3+} to Fe^{2+} by ascorbate present in the sample. Total
215 ascorbate plus dehydroascorbic acid content was measured by mixing the sample with 5mM
216 dithiothreitol (DTT) to reduce DHA, prior to the assay. Each extract was measured in duplicate.
217 The specificity of the assay has been checked by comparison with other known methods
218 (Stevens et al., 2006) and by using ascorbate oxidase to remove all ascorbate in order to
219 diminish other reductant background activity.

220 **Extraction of ascorbate degradation compounds, derivatization and analysis using GC-MS:**

221 Tomato leaves and fruit tissues were ground to powder in liquid nitrogen. Extraction was
222 performed in 1000µl of previously degassed cold methanol with 120µl of internal standard
223 ribitol (0.2mg.ml^{-1} in water). The mixture was extracted by mixing during 20 min at 4°C, and
224 then mixed vigorously with 400µl of water. After centrifugation at 12000 rpm, the supernatant
225 was reduced to dryness in a Speed-Vac. Samples were immediately analyzed or stored for a
226 maximum of 48h at -80°C. Dry residues were re-dissolved in 60µl of 20mg.ml^{-1} methoxyamine
227 in pyridine and derivatized for 90min at 37°C [carbonyl groups are transformed into the
228 corresponding oximes (methoximation)]. 8µl of retention time standards (a mixture of
229 dodecane, pentadecane, nonadecane, docosane) were added before trimethylsilylation.
230 MSTFA (N-methyl-N-trimethylsilyl-trifluoroacetamide; 120 µl) was then added and incubation
231 was continued for a further 30min at 37°C for trimethylsilylation (to increase volatility). Samples
232 were then loaded onto the AI 3000 autosampler. Sample volumes of 1µl were injected into the
233 GC column using a hot needle technique. Analyses were carried out with a Trace GC Ultra-
234 ISQ GC-MS system (Thermo France). Gas chromatography was performed on a Thermo TR-
235 5MS column (20m length x 0.10mm inner diameter x 0.10µm film thickness). The injection
236 temperature was set at 230°C and the ion source to 200°C. Helium was used as the carrier
237 gas at a flow rate of 0.4ml.min^{-1}. The following temperature schedule was set: 3.70 min
238 isothermal heating at 70°C, followed by a 7°C.min^{-1} ramp to reach 280°C and a second ramp
239 of 30°C/min to 320°C for a final heating of 1 min. Mass spectra were recorded at 6.6 scans.s^{-}
240 ^{1} with an *m*/*z* 50-650 scanning range. Mass spectra were cross-referenced with those in the
241 Golm Metabolome Database (Kopka et al., 2005). Relative concentrations were determined
242 by comparison with a ribitol internal standard.

243 **Statistical analysis:**

244 Data were submitted to a three-way analysis of variance (ANOVA) taking into account the
245 effect of genotype, environment and time and their interactions (XLStat software Addinsoft,
246 France). Significant differences between treatments were assessed by a Fisher's test ($p<0.05$).

247 **Results**

248 **Nature of ascorbate degradation compounds in tomato leaves**

249 As previous results have shown degradation at night (Conklin et al., 1997), a 24h time
250 course of sampling in darkness was carried out to assay catabolism of [^{14}C]ascorbate in the
251 leaflet laminae of detached tomato leaves. We used three extractants to detect and identify
252 different classes of ascorbate-derived compounds; in each case, the nature and quantity of the
253 radiolabelled compounds present in both the soluble and insoluble fractions were determined.
254 The radioactivity recovered in each fraction as a percentage of the total radioactivity is shown
255 in table 1. The small amount (<3%) of alkali-extractable material (extracted with NaOH after
256 formic acid treatment) was separated by dialysis into two parts: high and low molecular weight
257 (M_r). The proportion of alkali-extractable low-M_r material (potentially derived from polymer-
258 esterified oxalate and related substances) remained stable during the time course. Acid-
259 soluble radioactivity slightly decreased with time. Part of the radioactivity (up to 8.5% after 24h
260 of incubation) was trapped in the formic acid- and sodium hydroxide-insoluble pellet. Tests
261 with 2M TFA, an acid stronger than formic acid but whose volatility nevertheless facilitates its
262 use before HVPE, were carried out on the acid- and alkali-insoluble pellet in order to solubilise
263 calcium salts, notably [^{14}C]oxalate. After this extraction, and volatilization of TFA, a white
264 deposit was observed and HVPE of this deposit showed that no spot could be detected at the
265 origin point (Figure 1a), where the hypothetical calcium oxalate should appear (as it is not
266 mobile in HVPE). Two spots were detected and firstly labelled A and B (exhibiting an unusual
267 U-shape) as their nature was not revealed by appropriate markers run alongside (Figure 1a).
268 A and B were eluted, dried, mixed with orange G, and re-run at pH 6.5 before the paper
269 electrophoretograms were cut into strips of 1cm and assayed for ^{14}C by scintillation counting
270 (Figure 1b). Finally, the eluted sample of compound A was treated with NaOH and run at pH6.5
271 and it revealed its ability to inter-convert into two spots (Figure 3c). The strong hypothesis that
272 A and B are respectively compounds C and E (as named by Green and Fry, 2005b) is
273 supported by their mobility relative to the orange G marker and their ability to interconvert
274 (which is a peculiarity of the previously characterized compounds C and E). Thus, the two
275 spots were identified as carboxypentonates.

276 Characterization of the ascorbate-derived compounds in the formic acid-soluble
277 fraction was performed by HVPE analysis at pH 6.5 and pH2.0. At pH 6.5 (Figure 4a)
278 radioactive ascorbate derivatives are separated into: ascorbate and DKG (not clearly

279 separated), DHA, oxalyl threonate (OxT) and oxalate (OxA) predominantly, and small amounts
280 of compound E and proposed to be 2-carboxy-L-xylonate; Parsons et al., 2011). At pH2.0
281 (Figure 5a), ascorbate and DHA are not appreciably separated but cyclic oxalyl threonate
282 (cOxT), diketogulonate (DKG), compounds C and E, a mixture of oxalyl threonate isomers,
283 and oxalate were identifiable. The intensity of the radioactive bands (pH 2.0 and pH 6.5)
284 decreased for ascorbate, DHA and DKG over the time course while for oxalate, cyclic oxalyl
285 threonate and oxalyl threonate the spot intensity increased.

286 The percentage of [^{14}C]ascorbate and [^{14}C]DHA decreased rapidly during the first 8h
287 following incubation, giving evidence for the degradation of the ascorbate pool (Figure 4b). For
288 the next 16h of darkness, [^{14}C]ascorbate and [^{14}C]DHA decreased more slowly to reach
289 approximately 9% and 16% respectively of total radioactivity. Oxalyl threonates and oxalate
290 (soluble in cold formic acid, thus *not* the calcium salt) are the two major compounds that
291 increased during the time course. Oxalyl threonates and oxalate appeared simultaneously (as
292 observed *in vitro*; Parsons et al., 2011) to reach 30% and 25% of total formic acid-soluble
293 radioactivity respectively after 24h incubation. Compound E was also detected, and
294 accumulated slightly during the first 8h of the experiment, then decreased.

295 At pH2.0, the percentage of [^{14}C]ascorbate + DHA (Figure 5b) constantly decreased
296 during the time course from 70% to reach 30% of the soluble radioactivity. Oxalyl threonates,
297 oxalate and cyclic oxalyl threonate appeared simultaneously and increased constantly to reach
298 8%, 30% and 10% respectively after 24h. DKG, which was not resolved from ascorbate on
299 HVPE at pH 6.5, was clearly resolved at pH 2.0, and found to be abundantly present even at
300 the earliest time-point (11%), thereafter diminishing (to reach 2% of the total radioactivity).
301 Compounds C and E accumulated slightly during ascorbate metabolism (5% and 2% of total
302 radioactivity after 24h).

303 **Darkness activates degradation pathway independently of ascorbate pool size**

304 To complement these radiolabelling experiments, a GC-MS survey of two major
305 ascorbate degradation end-products, oxalate and threonate, was carried out on tomato leaves
306 subjected to different light and dark conditions. Tomato plantlets were grown under high light
307 conditions (1000 $\mu mol.m^{-2}.s^{-1}$) or low light conditions (100 $\mu mol.m^{-2}.s^{-1}$) for 7 days. A batch of
308 tomato plantlets was removed and stored for future analysis. A second batch of tomato
309 plantlets (from both conditions) was placed in darkness for 48h. Ascorbate and
310 dehydroascorbic acid content were assayed by spectrophotometric analysis. The content of
311 both was higher in high light plantlets than in low light plantlets (Table 2) after 7 days of the
312 different light treatments. During darkness, AsA and DHA decreased whereas oxalate and
313 threonate accumulated for plantlets previously grown under both low light and high light. The

314 ascorbic acid content decreased to 22–26% of its initial content (22% for initially low light
315 plantlets, 26% for initially high light plantlets). The oxidation product (DHA) also decreased, to
316 30% (high light) to 35% (low light) of its initial content after 48 hours of darkness.
317 Corresponding with the loss of both AsA and DHA, a 48-h dark period caused a substantial
318 increase in the products of irreversible DHA oxidation: OxA (5.4- fold in the initially high- and
319 low-light plants) and threonate (12.9- and 5-fold in the initially high- and low-light plants
320 respectively).

321 **Impact of a modification of MDHAR activity on degradation products**

322 The impact of a modification of MDHAR activity on ascorbate degradation was
323 evaluated using lines overexpressing or underexpressing MDHAR following the same HVPE
324 protocol as described above. Under darkness, we observed a slight decrease in the
325 accumulation of products from the DHA oxidation branch (i.e. oxalate and its esters) in
326 MDHAR-silenced lines compared to overexpressing lines and WT (significantly decreased
327 after 8h of incubation; Figure 6). No differences between lines were noticed for DHA hydrolysis
328 products (i.e. DKG and its downstream products). Similar results were observed by GC-MS
329 analysis on transgenic immature green fruits (Supplemental data Figure S1): OxA and
330 threonate accumulated less in silenced lines than in WT and overexpressing lines. However,
331 after 24h of metabolism, no difference between all genotypes could be detected (Table 3).

332 **A constant degradation rate under darkness**

333 Based on the accumulation of all degradation compounds and disappearance of
334 [^{14}C]ascorbate and DHA (of all lines mixed), we evaluated that 63% of total radioactivity
335 appeared in degradation products after 24h of darkness (Table 3). The degradation rate of
336 ascorbate was evaluated at 2.6% per hour. However, the dynamics of the degradation rate
337 might be not linear, as we observed that the first 8 hours of darkness are characterized by a
338 steep slope compared with the slope between 8h and 24h of darkness (Figure 4 and 5). The
339 degradation rate reported in 24h under darkness appears to be particularly constant during our
340 experiments (rates calculated on 2 to 5 independent leaflets per genotype).

341 ## Discussion

342 **Major oxidation products oxalate, threonate and oxalyl threonate are accumulated in tomato leaves in**
343 **darkness**

344 Characterization of soluble [1-^{14}C]ascorbate-derived compounds did not reveal any
345 compound related to tartrate metabolism in tomato leaves; thus the ascorbate → threonate →
346 tartrate pathway was not operative. Any tartrate formed via the L-idonate pathway ((i) in Figure
347 1) would not have included the ^{14}C of [1-^{14}C]ascorbate, and thus we would not have detected

348 it. However, we did detect DHA oxidation products: [^{14}C]oxalyl threonate, cyclic [^{14}C]oxalyl
349 threonate and [^{14}C]oxalate. For every [^{14}C]oxalate molecule formed, we can expect that one
350 non-radioactive threonate molecule is also produced during ascorbate degradation (via DHA),
351 following the stoichiometry of a 4-electron oxidation: [^{14}C]ascorbate $\rightarrow$ [^{14}C]oxalate + non-
352 radioactive threonate (Green and Fry, 2005b). Oxalyl threonate and cyclic oxalyl threonate are
353 alternative 4-electron oxidation products of ascorbate (Green & Fry 2005b; Parsons et al.,
354 2011). Oxalate and threonate are more stable, probably explaining why they are better-known
355 end-products of ascorbate degradation (Yang and Loewus, 1975). OxT and cOxT are
356 susceptible to enzymic hydrolysis, e.g. in plant cell-suspension cultures, by esterases which
357 are not yet fully characterised (Green & Fry, 2005b). In addition, there is evidence in plant cell
358 cultures for incompletely characterised enzymes that catalyse the oxidation of DHA (Green &
359 Fry, 2005b).

360 The DHA hydrolysis pathway initially yields DKG, which we detected transiently though
361 it later disappeared during the time-course. Low levels of compounds C and E, which are
362 proposed to be downstream carboxypentonates (2-carboxy-L-xylonolactone plus 2-carboxy-L-
363 lyxonolactone, and their common de-lactonisation product, respectively) arising from DKG
364 non-oxidatively (Parsons et al., 2011), were also detected in the formic acid extracts.
365 Production of such carboxypentonates *in vivo* is suggested to be highly dependent on
366 ascorbate concentration as residual ascorbate inhibits compound C formation but also on the
367 presence of H_2O_2 as highly oxidizing conditions divert DKG to oxidative pathways (Parsons et
368 al., 2011). Compounds C and E may not be metabolized further and appear to be quite stable
369 end-products of ascorbate degradation.

370 Up to 8.5% of the total radioactivity (after 24h in darkness) was inextractable by
371 consecutive treatments with formic acid and NaOH, but releasable from the NaOH-insoluble
372 fraction by TFA. Surprisingly, this radioactive material comprised mainly the
373 carboxypentonates (C and E) mentioned above (Figure 3). Their presence in the alkali-
374 insoluble fraction of tomato leaves is curious because compounds C and E are water-soluble
375 and would have been expected to be rapidly released by aqueous formic acid. Further
376 analyses could be carried out to investigate their potential biological role, as they represent up
377 to 8.5% of ascorbate labelling.

378 Some of the ascorbate degradation products from either DHA or DKG can contribute
379 to H_2O_2 release. This phenomenon can occur *in vivo* (Kärkönen and Fry, 2006). Furthermore,
380 oxalate could be enzymatically degraded (Foster et al., 2012), leading to form CO_2. In addition
381 to the compounds cited above, we suggest that H_2O_2 and CO_2 may have been released during
382 the experiment (but not measured).

383 **Decreasing MDHAR activity lowers the DHA oxidation rate**

384 It is worth noting that ascorbate recycling ensures a relatively high turnover rate of the
385 ascorbate pool, estimated at approximatively 13% per hour in pea seedlings (Pallanca and
386 Smirnoff, 2000). However, Haroldsen et al. (2011) showed that, in tomato fruits, DHAR and
387 MDHAR overexpression led to a depletion of the ascorbate pool. Similarly, the transgenic lines
388 studied in this paper overexpressing MDHAR also show a decrease in ascorbate levels in
389 leaves, and the silenced lines show an increase in ascorbate content both in leaves and fruits
390 (Gest et al., 2013), with no or slight effect on the DHA concentration. The activity of the isoform
391 3 of MDHAR, targeted in this study, is therefore negatively correlated to vitamin C (AsA + DHA)
392 content in tomato leaves, which is surprising since ascorbate is a product of MDHAR. These
393 results are not explained by changes in the expression of genes of the biosynthetic pathway,
394 or by changes in the activity of other enzymes involved in ascorbate recycling (DHAR and
395 glutathione reductase). The rate of DHA oxidation in these transgenic lines, reported in the
396 present manuscript, may offer a possible explanation for this ascorbate phenotype. Lines
397 silenced for MDHAR show a lower accumulation of irreversible degradation products (OxT,
398 oxalate, threonate etc.) in our experiments in darkness, agreeing with the higher ascorbate
399 content in leaves. Further experiments will be conducted in leaves and fruits to test if the DHA
400 oxidation rate could be partially under the control of MDHAR recycling enzyme or the MDHA
401 radical.

402 **Ascorbate pool size does not affect the percentage degradation rate of ascorbate in tomato leaves**

403 Smirnoff and Wheeler highlighted the D-mannose/L-galactose pathway as the main
404 biosynthetic pathway of ascorbate in plants (Wheeler et al., 1998). The recycling pathway
405 affects the redox state of the ascorbate pool and is especially important during stress
406 responses (Noctor and Foyer, 1998). Light intensity and light quality are the prominent
407 environmental factors influencing ascorbate biosynthesis and recycling (Li et al., 2009; Massot
408 et al., 2012). The degradation rate of ascorbate in different light environments had never been
409 studied before in tomato leaves. We found higher ascorbate content in plantlets kept under
410 high light than those grown under low light in line with current observations on the activation
411 of synthesis and recycling by light (Bartoli et al., 2006; Gautier et al., 2008). Oxalate and
412 threonate increased during darkness but not during high light stress or low light treatment. In
413 the light, oxalate and threonate do not accumulate but this does not mean that degradation
414 does not take place in the light as oxalate oxidase may be light-promoted as mentioned above
415 (Loewus, 1999). Ascorbate levels of high light and low light plantlets were not similar at the
416 beginning of the darkness treatment but the quantity of degradation products was proportional
417 to the size of the total ascorbate pool (representing 20% of the initial content after 48h). If we

418 consider the final concentration of the vitamin C pool (AsA+DHA) after 48h of treatment, it
419 represents 56% of the initial content. The degradation rate under darkness could be evaluated
420 at about 1.5% per hour. This result is comparable to those obtained by (Conklin et al., 1997)
421 on *Arabidopsis* where 40% of ascorbate degraded in the dark during 24h in *Arabidopsis*
422 detached leaves. However, if we consider the fact that GC-MS analysis does not allow the
423 detection of oxalyl-threonate, cyclic-oxalyl-threonate, DKG and carboxypentonates (thus,
424 supporting the choice of HVPE analysis), this result is clarified by those obtained using
425 radiolabelled experiments, where we noticed a degradation rate of about 2.6% per hour. The
426 fate of the abundant DKG, observed at 1 h (Figure 5a), is unclear; it is possible that some of
427 the [1-^{14}C]DKG was oxidatively decarboxylated to $^{14}CO_2$ plus a non-radioactive C_5 product
428 such as 2-keto-L-xylonate, as observed *in vitro* (Deutsch, 1998; Parsons and Fry, 2012).
429 Products mostly coming from DHA oxidation accumulated in the dark compared to those
430 coming from DKG (the product of DHA hydrolysis), which remained at 5 to 10 % of radioactivity
431 measured following the first hour of incubation. These products did not accumulate in the
432 soluble fraction during ascorbate degradation under darkness, but might be trapped into
433 insoluble material as mentioned above.

434 These multiple experiments support the hypothesis that the percentage degradation
435 rate in darkness is stable over 24h in tomato leaves, whatever the ascorbate content is at the
436 beginning of the darkness period.

437 **Conclusions**

438 Ascorbate degradation in the light or dark was studied in tomato leaves. Oxalate, threonate
439 and oxalyl threonate were identified as end-products of ascorbate degradation (DHA oxidation
440 branch). No tartaric acid was detected. The degradation rate was evaluated at 63% after 24h
441 in dark conditions, with a major part of the degradation coming from DHA oxidation rather than
442 via DKG (DHA hydrolysis). Carboxypentonates were also detected and trapped through
443 unidentified bonding in the insoluble (cell wall-rich) leaf material. Further analysis will be
444 performed to highlight their potential biological role. The percentage degradation rate is
445 independent of the initial ascorbate level over periods of 24h and is under environmental
446 control. In order to understand how to increase or stabilize ascorbate content in plants and
447 fruits, controlling the degradation rate could be a good solution as degradation of ascorbate is
448 non-reversible, and control of MDHAR activity may be a solution to explore. Efficient ascorbate
449 recycling will also enhance protection of the ascorbate pool from degradation.

450 **Acknowledgements**

The authors declare that there are no conflicts of interest. We are grateful to the greenhouse experimental crew of Edinburgh University, and to Janice Miller and Rebecca Dewhirst for their helpful assistance in radiolabelling and electrophoresis experiments. We thank Gisele Riqueau for her technical assistance at INRA Avignon. The PhD of Vincent Truffault was financed by INRA and the Provence-Alpes-Côte d'Azur region. We thank Académie d'Agriculture de France for the funding of the stay of Vincent Truffault in the Edinburgh Cell Wall Group. SCF thanks the UK Biotechnology and Biological Sciences Research Council (BBSRC) and Vitacress Salads Ltd for financial support.

459 **References**

460 **Bartoli, C.G., Yu, J., Gómez, F., Fernández, L., McIntosh, L. and Foyer, C.H.** (2006) Inter-
461 relationships between light and respiration in the control of ascorbic acid synthesis and
462 accumulation in Arabidopsis thaliana leaves. *J. Exp. Bot.*, **57**, 1621–1631.

463 **Conklin, P.L., Pallanca, J.E., Last, R.L. and Smirnoff, N.** (1997) L-Ascorbic acid metabolism
464 in the ascorbate-deficient Arabidopsis mutant *vtc1*. *Plant Physiol.*, **115**, 1277–1285.

465 **DeBolt, S., Cook, D.R. and Ford, C.M.** (2006) L-Tartaric acid synthesis from vitamin C in
466 higher plants. *PNAS*, **103**, 5608–5613.

467 **DeBolt, S., Hardie, J., Tyerman, S. and Ford, C.M.** (2004) Composition and synthesis of
468 raphide crystals and druse crystals in berries of Vitis vinifera L. cv. Cabernet Sauvignon:
469 Ascorbic acid as precursor for both oxalic and tartaric acids as revealed by radiolabelling
470 studies. *Australian Journal of Grape and Wine Research*, **10**, 134–142.

471 **Deutsch, J.C.** (1998) Oxygen-accepting antioxidants which arise during ascorbate oxidation.
472 *Analytical Biochemistry*, **265**, 238–245.

473 **Dowdle, J., Ishikawa, T., Gatzek, S., Rolinski, S. and Smirnoff, N.** (2007) Two genes in
474 Arabidopsis thaliana encoding GDP-L-galactose phosphorylase are required for ascorbate
475 biosynthesis and seedling viability: Role of GDP-l-Gal phosphorylase in ascorbate
476 biosynthesis. *The Plant Journal*, **52**, 673–689.

477 **Dumville, J.C. and Fry, S.C.** (2003) Solubilisation of tomato fruit pectins by ascorbate: a
478 possible non-enzymic mechanism of fruit softening. *Planta*, **217**, 951–961.

479 **Foster, J., Kim, H.U., Nakata, P.A. and Browse, J.** (2012) A previously unknown oxalyl-CoA
480 synthetase is important for oxalate catabolism in Arabidopsis. *Plant Cell*, **24**, 1217–1229.

481 **Franceschi, V.R. and Nakata, P.A.** (2005) Calcium oxalate in plants: formation and function.
482 *Annual Review of Plant Biology*, **56**, 41–71.

483 **Fry, S.C.** (2011) High-voltage paper electrophoresis (HVPE) of cell-wall building blocks and
484 their metabolic precursors. In Z. A. Popper, ed. *The Plant Cell Wall*. Totowa, NJ: Humana
485 Press, pp. 55–80.

486 **Fry, S.C.** (1998) Oxidative scission of plant cell wall polysaccharides by ascorbate-induced
487 hydroxyl radicals. *Biochemical Journal*, **332**, 507–515.

488 **Gautier, H., Diakou-Verdin, V., Bénard, C., Reich, M., Buret, M., Bourgaud, F., Poëssel,**
489 **J.L., Caris-Veyrat, C. and Génard, M.** (2008) How does tomato quality (sugar, acid, and
490 nutritional quality) vary with ripening stage, temperature, and irradiance? *J. Agric. Food Chem.*,
491 **56**, 1241–1250.

492 **Gest, N., Garchery, C., Gautier, H., Jiménez, A. and Stevens, R.** (2013) Light-dependent
493 regulation of ascorbate in tomato by a monodehydroascorbate reductase localized in
494 peroxisomes and the cytosol. *Plant Biotechnology Journal*, **11**, 344–354.

495 **Giovanelli, J.** (1966) Oxalyl-coenzyme A synthetase from pea seeds. *Biochimica et*
496 *Biophysica Acta (BBA) - Enzymology and Biological Oxidation*, **118**, 124–143.

497 **Green, M.A. and Fry, S.C.** (2005) Apoplastic degradation of ascorbate: Novel enzymes and
498 metabolites permeating the plant cell wall. *Plant Biosystems*, **139**, 2–7.

499 **Green, M.A. and Fry, S.C.** (2005) Vitamin C degradation in plant cells via enzymatic hydrolysis
500 of 4-*O*-oxalyl-L-threonate. *Nature*, **433**, 83–87.

Hamner, K.C., Bernstein, L. and Maynard, L.A. (1945) Effects of light intensity, day length, temperature, and other environmental factors on the ascorbic acid content of tomatoes. *J. Nutr.*, **29**, 85–97.

Hancock, R.D. and Viola, R. (2005) Biosynthesis and catabolism of L-ascorbic acid in plants. *Critical Reviews in Plant Sciences*, **24**, 167–188.

Hellman, L. and Burns, J.J. (1958) Metabolism of L-ascorbic acid-1-^{14}C in man. *J. Biol. Chem.*, **230**, 923–930.

Haroldsen, V. M., Chi-Ham, C. L., Kulkarni, S., Lorence, A., & Bennett, A. B. (2011) Constitutively expressed DHAR and MDHAR influence fruit, but not foliar ascorbate levels in tomato. *Plant Physiology and Biochemistry*, **49**, 1244-1249.

Helsper, J.P. and Loewus, F.A. (1982) Metabolism of L-threonic acid in *Rumex* x *acutus* L. and *Pelargonium crispum* (L.) L'Hér. *Plant Physiol.*, **69**, 1365–1368.

Kärkönen, A. and Fry, S.C. (2006) Effect of ascorbate and its oxidation products on H_2O_2 production in cell-suspension cultures of *Picea abies* and in the absence of cells. *J. Exp. Bot.*, **57**, 1633–1644.

Kay, P., Wagner, J.R., Gagnon, H., Day, R. and Klarskov, K. (2013) Modification of peptide and protein cysteine thiol groups by conjugation with a degradation product of ascorbate. *Chem. Res. Toxicol.*, **26**, 1333–1339.

Khan, S.R. (1995) *Calcium Oxalate in Biological Systems*, CRC Press.

Kopka, J., Schauer, N., Krueger, S., et al. (2005) GMD@CSB.DB: the Golm Metabolome Database. *Bioinformatics*, **21**, 1635–1638.

Laing, W.A., Martínez-Sánchez, M., Wright, M.A., et al. (2015) An upstream open reading frame is essential for feedback regulation of ascorbate biosynthesis in Arabidopsis. *The Plant Cell*, **27**, 772–786.

Lane, B.G. (1994) Oxalate, germin, and the extracellular matrix of higher plants. *FASEB J*, **8**, 294–301.

Li, M., Ma, F., Shang, P., Zhang, M., Hou, C. and Liang, D. (2009) Influence of light on ascorbate formation and metabolism in apple fruits. *Planta*, **230**, 39–51.

Libert, B. and Franceschi, V.R. (1987) Oxalate in crop plants. *J. Agric. Food Chem.*, **35**, 926–938.

Lin, L.-S. and Varner, J.E. (1991) Expression of ascorbic acid oxidase in zucchini squash (*Cucurbita pepo* L.). *Plant Physiol.*, **96**, 159–165.

Linster, C.L. and Van Schaftingen, E. (2007) Vitamin C: Biosynthesis, recycling and degradation in mammals. *FEBS Journal*, **274**, 1–22.

Loewus, F.A. (1999) Biosynthesis and metabolism of ascorbic acid in plants and of analogs of ascorbic acid in fungi. *Phytochemistry*, **52**, 193–210.

Massot, C., Bancel, D., Lopez Lauri, F., Truffault, V., Baldet, P., Stevens, R. and Gautier, H. (2013) High temperature inhibits ascorbate recycling and light stimulation of the ascorbate pool in tomato despite increased expression of biosynthesis genes. *PLoS ONE*, **8**, e84474.

Massot, C., Stevens, R., Génard, M., Longuenesse, J.-J. and Gautier, H. (2011) Light affects ascorbate content and ascorbate-related gene expression in tomato leaves more than in fruits. *Planta*, **235**, 153–163.

Melino, V.J., Soole, K.L. and Ford, C.M. (2009) Ascorbate metabolism and the developmental demand for tartaric and oxalic acids in ripening grape berries. *BMC Plant Biol*, **9**, 145.

Muller, K., Linkies, A., Vreeburg, R.A.M., Fry, S.C., Krieger-Liszkay, A. and Leubner-Metzger, G. (2009) In vivo cell wall loosening by hydroxyl radicals during cress seed germination and elongation growth. *Plant physiology*, **150**, 1855–1865.

Nakata, P.A. (2003) Advances in our understanding of calcium oxalate crystal formation and function in plants. *Plant Science*, **164**, 901–909.

Nakata, P.A. (2012) Plant calcium oxalate crystal formation, function, and its impact on human health. *Frontiers in biology*, **7**, 254–266.

Nakata, P.A. and McConn, M.M. (2003) Influence of the calcium oxalate defective 4 (cod4) mutation on the growth, oxalate content, and calcium content of *Medicago truncatula*. *Plant Science*, **164**, 617–621.

Nemet, I. and Monnier, V.M. (2011) Vitamin C degradation products and pathways in the human lens. *J. Biol. Chem.*, **286**, 37128–37136.

Noctor, G. and Foyer, C.H. (1998) Ascorbate and glutathione: Keeping active oxygen under control. *Annual Review of Plant Physiology and Plant Molecular Biology*, **49**, 249–279.

Pallanca, J. E., & Smirnoff, N. (2000) The control of ascorbic acid synthesis and turnover in pea seedlings. *Journal of Experimental Botany*, **51**, 669-674.

Parsons, H.T. and Fry, S.C. (2012) Oxidation of dehydroascorbic acid and 2,3-diketogulonate under plant apoplastic conditions. *Phytochemistry*, **75**, 41–49.

Parsons, H.T., Yasmin, T. and Fry, S.C. (2011) Alternative pathways of dehydroascorbic acid degradation in vitro and in plant cell cultures: novel insights into vitamin C catabolism. *Biochemical Journal*, **440**, 375–385.

Regulus, P., Desilets, J.-F., Klarskov, K. and Wagner, J.R. (2010) Characterization and detection in cells of a novel adduct derived from the conjugation of glutathione and dehydroascorbate. *Free Radical Biology and Medicine*, **49**, 984–991.

Simpson, G.L.. and Ortwerth, B.. (2000) The non-oxidative degradation of ascorbic acid at physiological conditions. *Biochimica et Biophysica Acta (BBA) - Molecular Basis of Disease*, **1501**, 12–24.

Smirnoff, N. and Wheeler, G.L. (2000) Ascorbic acid in plants: Biosynthesis and function. *Critical Reviews in Biochemistry and Molecular Biology*, **35**, 291–314.

Stevens, R., Buret, M., Garchery, C., Carretero, Y. and Causse, M. (2006) Technique for rapid, small-scale analysis of vitamin C levels in fruit and application to a tomato mutant collection. *J. Agric. Food Chem.*, **54**, 6159–6165.

Tooulakou, G., Giannopoulos, A., Nikolopoulos, D., et al. (2016) “Alarm photosynthesis”: calcium oxalate crystals as an internal CO_2 source in plants. *Plant Physiol.*, pp.00111.2016.

Wagner, G. and Loewus, F. (1973) The biosynthesis of (+)-tartaric acid in *Pelargonium crispum*. *Plant Physiol.*, **52**, 651–654.

582 **Wheeler, G.L., Jones, M.A. and Smirnoff, N.** (1998) The biosynthetic pathway of vitamin C
583 in higher plants. *Nature*, **393**, 365–369.

584 **Yang, J.C. and Loewus, F.A.** (1975) Metabolic conversion of L-ascorbic acid to oxalic acid in
585 oxalate-accumulating plants. *Plant Physiol.*, **56**, 283–285.

586 **Yew, W.S. and Gerlt, J.A.** (2002) Utilization of L-ascorbate by Escherichia coli K-12:
587 Assignments of functions to products of the yjf-sga and yia-sgb operons. *J. Bacteriol.*, **184**,
588 302–306.

589 **Yu, L., Jiang, J., Zhang, C., et al.** (2010) Glyoxylate rather than ascorbate is an efficient
590 precursor for oxalate biosynthesis in rice. *J. Exp. Bot.*, **61**, 1625–1634.

591 **Table 1**: Distribution of ^{14}C in detached tomato leaves between formic acid- and NaOH-
592 extractable pools and the NaOH-inextractable residue after incubation with [1-^{14}C]ascorbate in
593 darkness. Detached leaves were incubated for 60min with the cut petiole in radioactive solution
594 then the leaves were transferred such that the petiole was in water for the next 24h. Results
595 are expressed as percentage of the total radioactivity detected in the tomato lamina. Acid
596 extraction included 15% formic acid homogenization followed by centrifugation. Basic
597 extraction was performed by adding 1M NaOH to the pellet after acid extraction. 'Soluble
598 polymers' were detected in the alkali extract by dialysis. NaOH-inextractable radioactivity was
599 solubilised in cold 2M TFA of the NaOH-resistant pellet.

	% of total radioactivity after			
	1h	**4h**	**6h**	**24h**
$SC_{(1)}$ **Acid extraction**	95	93	92	88
$SC_{(2)}$ **Basic extraction**	2	3	3	3
$SC_{(3)}$ **NaOH-soluble polymers**	0.02	0.04	0.05	0.10
$SC_{(4)}$ **NaOH-inextractable radioactivity**	3	4	5	9
$SC_{(5)}$ **Pellet**	≈0	≈0	≈0	≈0

600

601 **Table 2**: Ascorbate (AsA), dehydroascorbic acid (DHA) and their oxidative end-products
602 oxalate (OxA) and threonate (ThrO) in tomato leaves grown under high light (1000 µmol.m^{-2}.s^{-1}
603) or low light (100 µmol.m^{-2}.s^{-1}), and after 48h of subsequent complete darkness. OxA and
604 ThrO were assayed by GC-MS analysis and expressed in arbitrary unit.gFw^{-1}. Ascorbate and
605 DHA content were assayed by spectrophotometric analysis and expressed in mg.100gFw^{-1}.
606 Six replicates (independent plantlets) per condition were used. Different letters indicate
607 significant differences (p<0.05).

	mg.100gFw^{-1}				*arbitrary unit.gFw^{-1}*		*arbitrary unit.gFw^{-1}*	
	AsA	p<0.05	**DHA**	p<0.05	**OxA**	p<0.05	**ThrO**	p<0.05
high light	127.9	*a*	26.7	*a*	8.9	*c*	1.3	*b*
48h dark	33.1	*b*	8.0	*b*	48.0	*a*	16.8	*a*
low light	41.8	*b*	8.5	*b*	5.7	*c*	0.5	*b*
48h dark	9.0	*c*	3.0	*c*	30.6	*b*	2.5	*b*

608

609 **Table 3**: Repartition of the radioactivity after 24h of [^{14}C]ascorbate metabolism in darkness in
610 different transgenic lines modified for their MDHAR activity. Lines under-expressing MDHAR
611 are mds42 and mds5, overexpressing lines are sx1.7 and sx6.10. Wild type (WT) is used as
612 reference. The Table shows scintillation counts of total soluble radioactivity in degradation
613 products and in ascorbate and dehydroascorbic acid pool. Results (mean ± standard deviation)
614 are expressed as percentage of total soluble radioactivity. 5 replicates for WT, sx6.10 and
615 mds42; 2 replicates for sx1.7 and mds5 lines were used. No significant difference ($p<0.1$) was
616 detected between genotypes.

	% of 14C recovered in AsA+DHA after 24h	p<0.1	**% of 14C recovered in degradation products after 24h**	p<0.1
WT	37 ±6.2	a	63 ±9.9	a
mds42	37 ±11.7	a	63 ±18.7	a
mds5	43 ±2.8	a	57 ±2.8	a
sx1.7	30 ±3.3	a	70 ±3.3	a
sx6.10	41 ±4.2	a	59 ±1.5	a

617

618 **Figure legends**

619 **Figure 1**: Ascorbate degradation pathways identified in (i) Vitaceae (tartaric acid pathway), (ii)
620 Geraniaceae and cultured *Rosa* cells (DHA oxidative pathway), (iii) cultured *Rosa* cells (DHA
621 hydrolysis pathway), (iv) *Pelargonium crispum*; (vii) mammals, (viii) human lens and (ix)
622 bacteria. (v) has been reported mostly in monocots; (vi) in *Arabidopsis*, pea, pumpkin and lupin
623 seeds and wheat germ. Enzymes except L-IdnDH (L-idonate dehydrogenase), AO (ascorbate
624 oxidase), APX (ascorbate peroxidase), MDHAR (monodehydroascorbate reductase), DHAR
625 (dehydroascorbate reductase), oxalate oxidase, oxalyl-CoA synthetase and esterase from
626 oxalate pathway and those of the bacteria degradation pathway (not indicated here) are not
627 required or are yet unidentified. Adapted from (i) DeBolt et al., 2004, 2006; Melino et al., 2009
628 (ii) Green & Fry, 2005b; Parsons et al., 2011 (iii) Parsons et Fry, 2012 (iv) Wagner and Loewus,
629 1973 (v) Loewus, 1999 (vi) Foster et al., 2012 (vii) Linster and Van Schaftingen, 2007; Simpson
630 and Ortwerth, 2000, Nemet and Monnier, 2011 (viii) Nemet and Monnier, 2011 and (ix) Yew
631 and Gerlt, 2002.

632 **Figure 2**: Flow chart of the methodology used to localize radioactivity within the leaflet lamina
633 tissue. HVPE is for high voltage paper electrophoresis and SC is for scintillation counting. Each
634 extraction was conducted as described in materials and methods. Results of $SC_{(1, 2, 3, 4, 5)}$ are
635 shown in Table 1.

636 **Figure 3**: (a) Accumulation of alkali-inextractable [1-^{14}C]ascorbate derivatives in tomato leaves
637 under darkness. After acidic and basic extraction as described in figure 2, samples of the TFA-
638 solubilised, NaOH-insoluble material were dried on Whatman paper No.3 and electrophoresed
639 in a volatile buffer at pH6.5 (acetic acid-pyridine-water, 1:33:300 by volume, containing 5mM
640 EDTA) for 30min at 3.0kV. Spots on the autoradiogram were not identified by comparison with
641 non-radioactive markers run alongside. (b) A and B were eluted, dried, mixed with Orange G,
642 and re-run at pH 6.5 (as described in (a)) before paper electrophoretograms were cut into strips
643 of 1cm and assayed for ^{14}C by scintillation counting. (c) Eluted fraction of compound A was
644 treated with NaOH and ran at pH6.5 (as described in (a)). Streaks were compared to
645 compound A untreated.
646 Compounds A and B are believed to be lactonised (compound C) and de-lactonised
647 (compound E) carboxypentonates respectively (Parsons et al., 2011).

648 **Figure 4**: Fate of [^{14}C]ascorbate in wild-type tomato leaves in the dark: analysis by HVPE at
649 pH 6.5. (a) After a 1-h pulse of [1-^{14}C]ascorbate fed to tomato leaves via the cut petiole,
650 followed by a chase of up to 24 h in non-radioactive water, metabolites were extracted from
651 leaflets with formic acid and analysed by HVPE at pH 6.5. An autoradiograph is shown. Spots
652 are identified by reference to stained markers.

653 (b) Quantification of the radioactive spots by scintillation counting. AsA, DHA and DKG-
654 derivatives are shown as white symbols; downstream metabolites are shown as black symbols:
655 oxalyl threonate (OxT) and oxalate (OxA). Results are expressed as percentage of total
656 HCOOH-soluble radioactivity.

657 **Figure 5**: Fate of [^{14}C]ascorbate in wild-type tomato leaves in the dark: analysis by HVPE at
658 pH 2.0.
659 Other experimental details as in Fig. 4. Ascorbate (AsA) and dehydroascorbic acid (DHA) are
660 both essentially uncharged at pH 2, resulting in a single radioactive spot near the origin.

661 **Figure 6**: Accumulation of degradation products derived from [^{14}C]ascorbate (similar protocol
662 to that of figure 3) in leaves of different transgenic lines modified for their MDHAR activity. The
663 graph shows lines under-expressing MDHAR (mds; white symbols), overexpressing lines (sx;
664 grey symbols), and wild type (WT; black symbols). Scintillation counts of total soluble
665 radioactivity in products coming from DHA oxidation (OxT, cOxT, OxA; triangles) and via DHA
666 hydrolysis (DKG, C, E; circles) during 24h of dark incubation with [1-^{14}C]ascorbate are shown.
667 Results (mean ± standard deviation) are expressed as percentage of total formic acid-soluble
668 radioactivity. Six replicates for sx and mds lines and 4 for WT line were used. One star indicates
669 a significant difference from the wild type WT ($p<0.07$).

670 **Supplemental data legends**

671 **Supplemental data Figure S1**: Oxalate (OxA) and threonate (ThrO) content in green tomato
672 fruits of transgenic lines modified for their MDHAR activity. mds3 and mds5 are two
673 independent lines under-expressing MDHAR (hatched bars). sx1.7 and sx6.10 are two
674 independent lines overexpressing MDHAR (grey bars). Wild type (WT) is used as reference
675 (white bar). Oxalate (OxA) and threonate (ThrO) were assayed by GC-MS and expressed in
676 arbitrary unit/gFw. Five replicates were used per genotype. Different letters indicate significant
677 differences ($p<0.05$).

Fig. 1

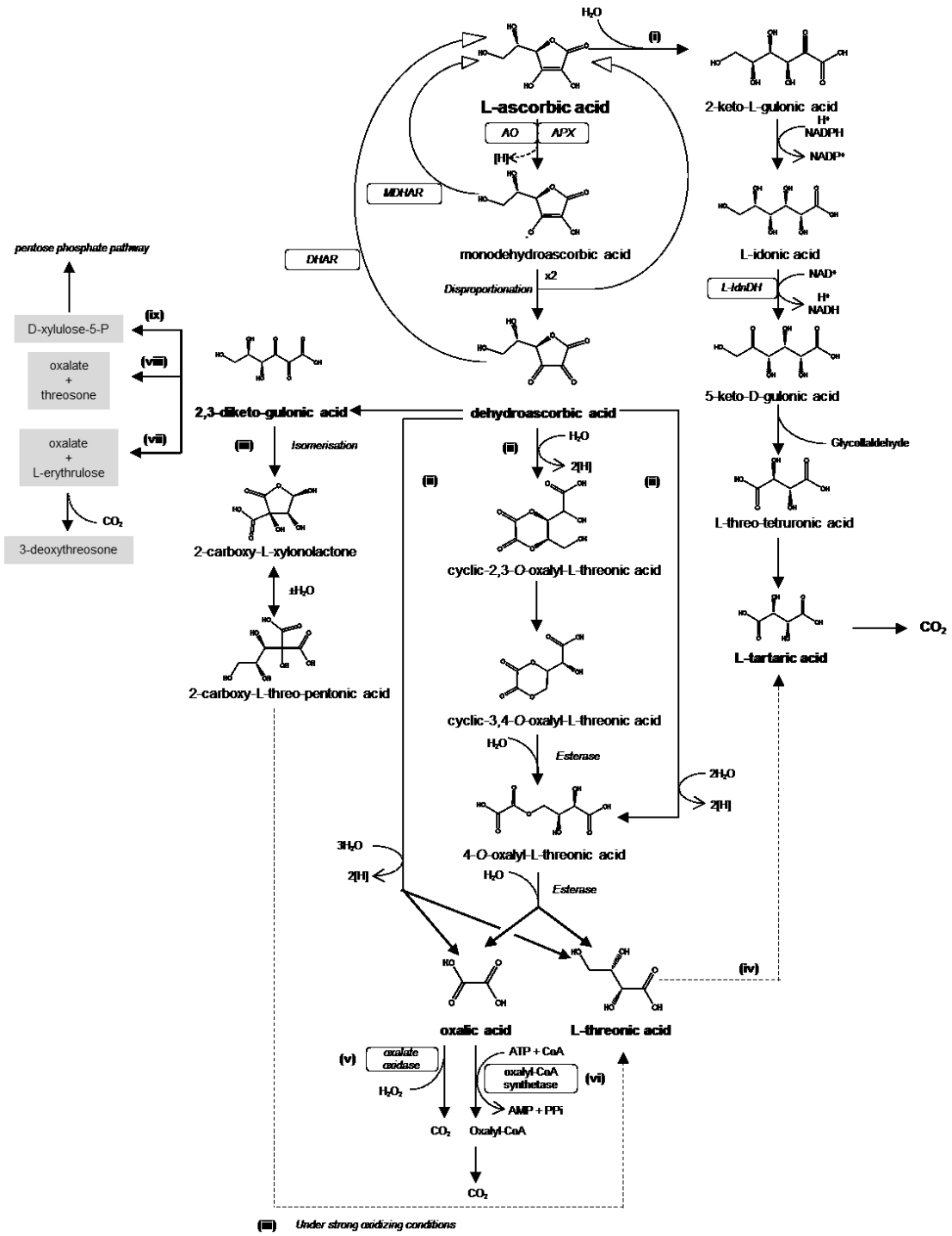
L-ascorbic acid
AO
APX
[H]
MDHAR
DHAR
monodehydroascorbic acid
Disproportionation
x2
dehydroascorbic acid
H2O
(i)
2-keto-L-gulonic acid
H+
NADPH
NADP+
L-idonic acid
L-IdnDH
NAD+
H+
NADH
5-keto-D-gulonic acid
Glycollaldehyde
L-threo-tetruronic acid
L-tartaric acid
CO2
pentose phosphate pathway
D-xylulose-5-P
oxalate + threosone
oxalate + L-erythrulose
3-deoxythreosone
(ix)
(viii)
(vii)
2,3-diketo-gulonic acid
(iii)
Isomerisation
2-carboxy-L-xylonolactone
±H2O
2-carboxy-L-threo-pentonic acid
(ii)
2[H]
cyclic-2,3-O-oxalyl-L-threonic acid
cyclic-3,4-O-oxalyl-L-threonic acid
Esterase
2H2O
4-O-oxalyl-L-threonic acid
3H2O
oxalic acid
L-threonic acid
(iv)
(v)
oxalate oxidase
H2O2
ATP + CoA
oxalyl-CoA synthetase
(vi)
AMP + PPi
Oxalyl-CoA
(iii) Under strong oxidizing conditions

Fig. 2

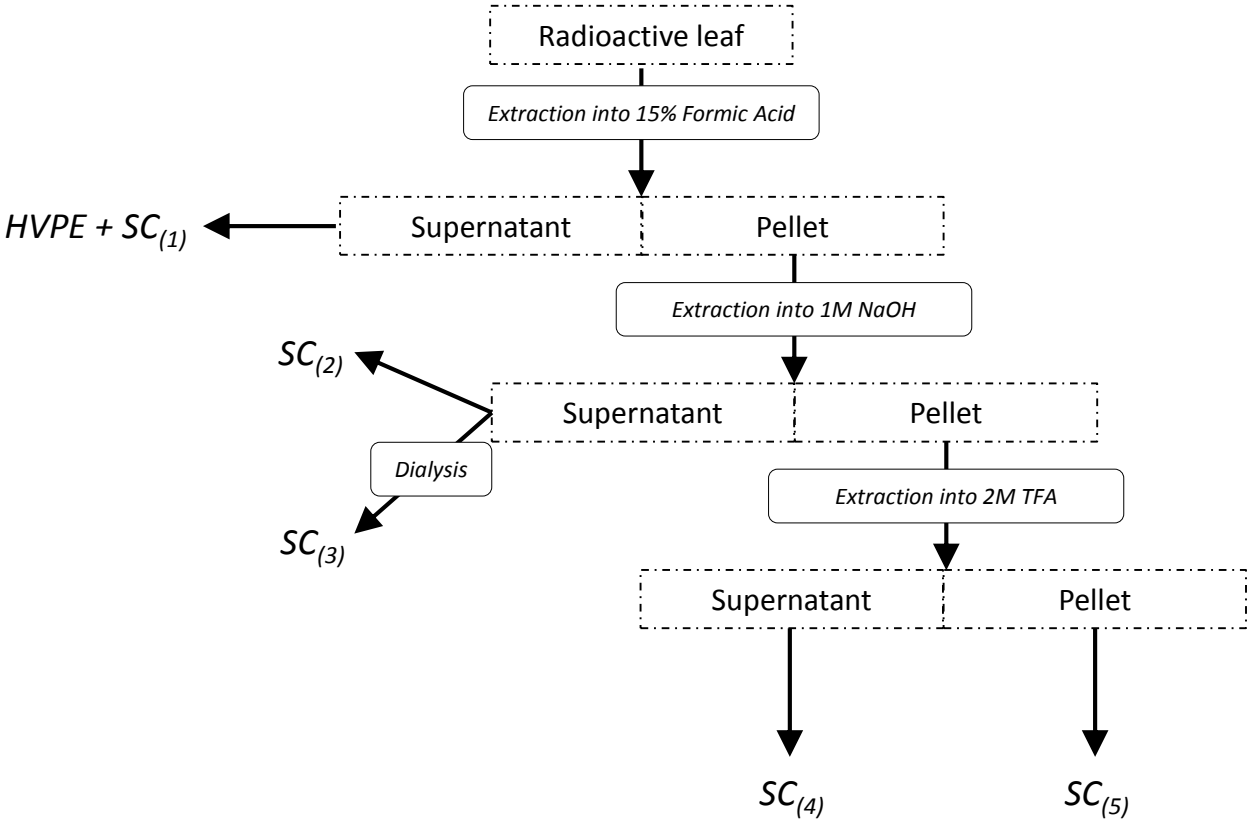
Radioactive leaf
Extraction into 15% Formic Acid
HVPE + SC(1)
Supernatant
Pellet
Extraction into 1M NaOH
SC(2)
Supernatant
Pellet
Dialysis
SC(3)
Extraction into 2M TFA
Supernatant
Pellet
SC(4)
SC(5)

Table 1

	% of total radioactivity after			
	1h	**4h**	**6h**	**24h**
$SC_{(1)}$ **Acid extraction**	95	93	92	88
$SC_{(2)}$ **Basic extraction**	2	3	3	3
$SC_{(3)}$ **NaOH-soluble polymers**	0.02	0.04	0.05	0.10
$SC_{(4)}$ **NaOH-inextractable radioactivity**	3	4	5	9
$SC_{(5)}$ **Pellet**	≈0	≈0	≈0	≈0

Fig. 3

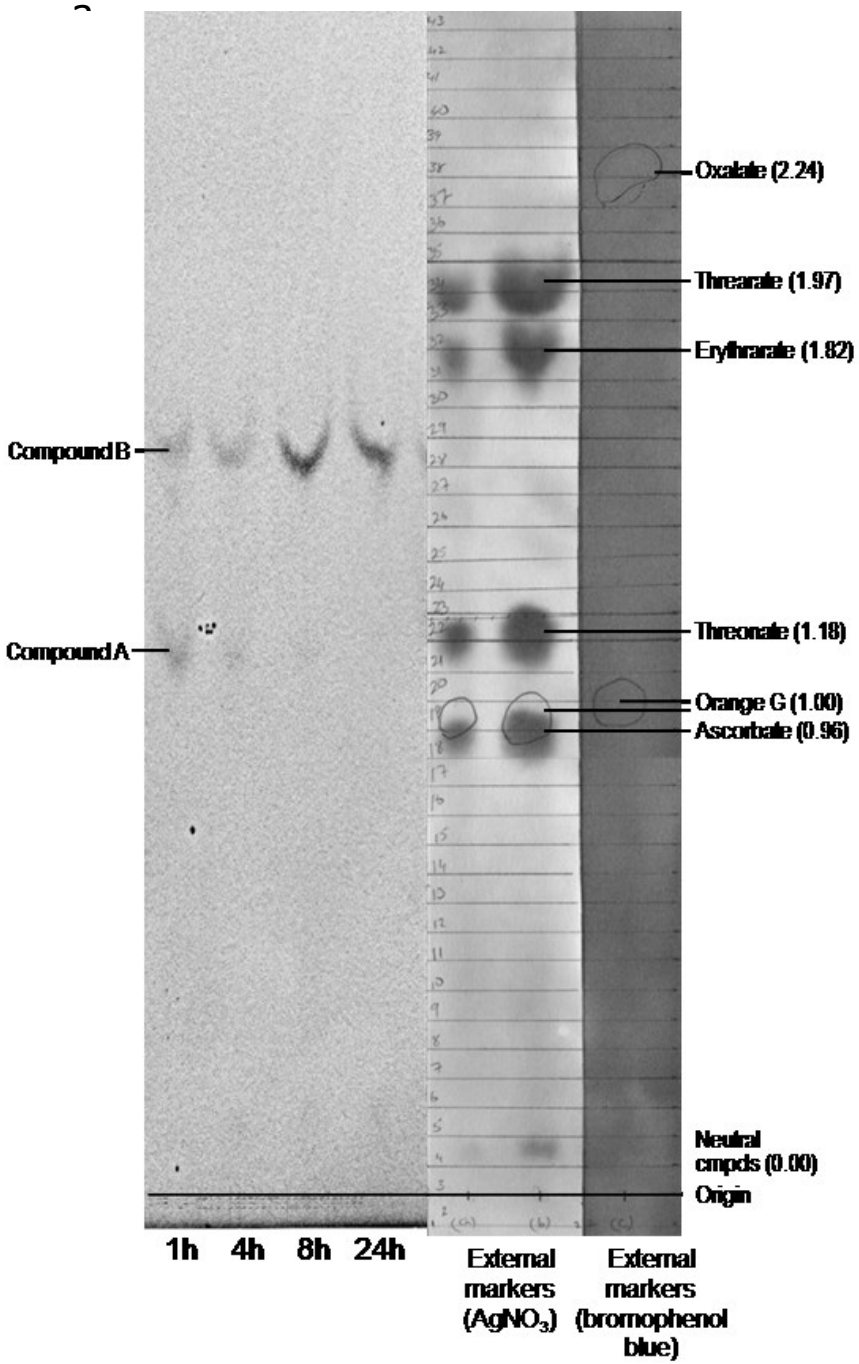
Oxalate (2.24)
Threarate (1.97)
Erythrarate (1.82)
Compound B
Compound A
Threonate (1.18)
Orange G (1.00)
Ascorbate (0.96)
Neutral cmpds (0.00)
Origin
1h
4h
8h
24h
External markers ($AgNO_3$)
External markers (bromophenol blue)

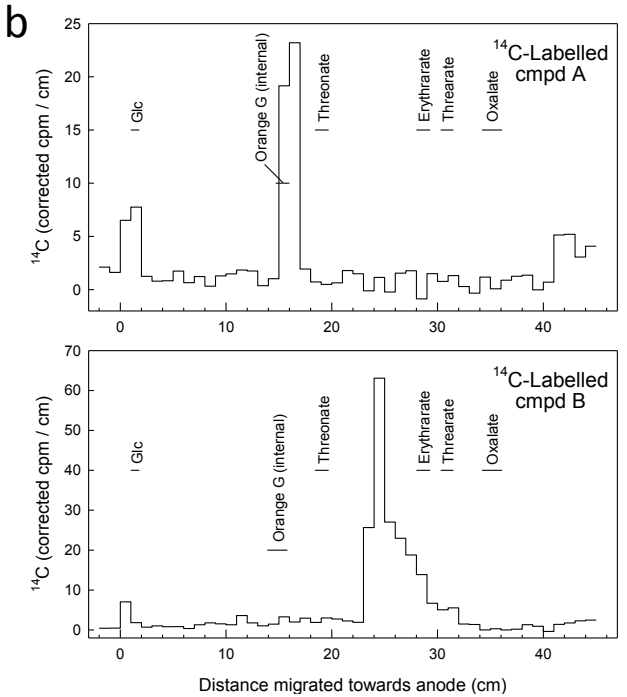
b
^{14}C-Labelled cmpd A
^{14}C-Labelled cmpd B
Glc
Orange G (internal)
Threonate
Erythrarate
Threarate
Oxalate
^{14}C (corrected cpm / cm)
Distance migrated towards anode (cm)

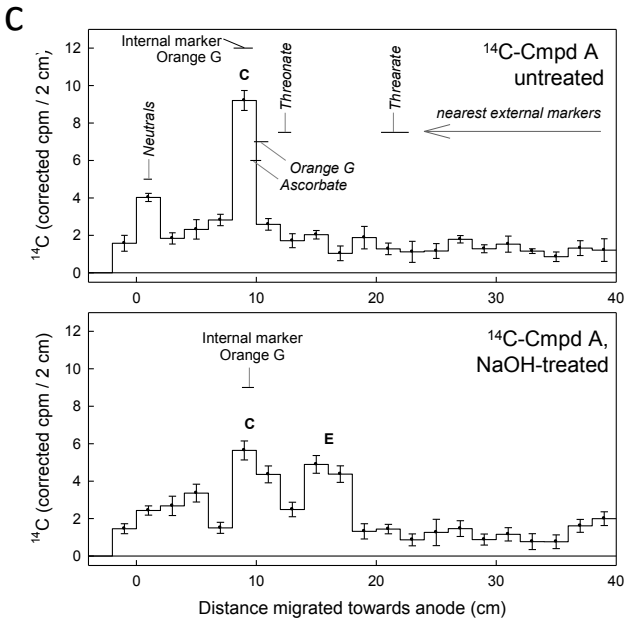
c
^{14}C-Cmpd A untreated
^{14}C-Cmpd A, NaOH-treated
Internal marker Orange G
Neutrals
Threonate
Threarate
nearest external markers
Orange G
Ascorbate
C
E
^{14}C (corrected cpm / 2 cm)
Distance migrated towards anode (cm)

Fig. 4

a

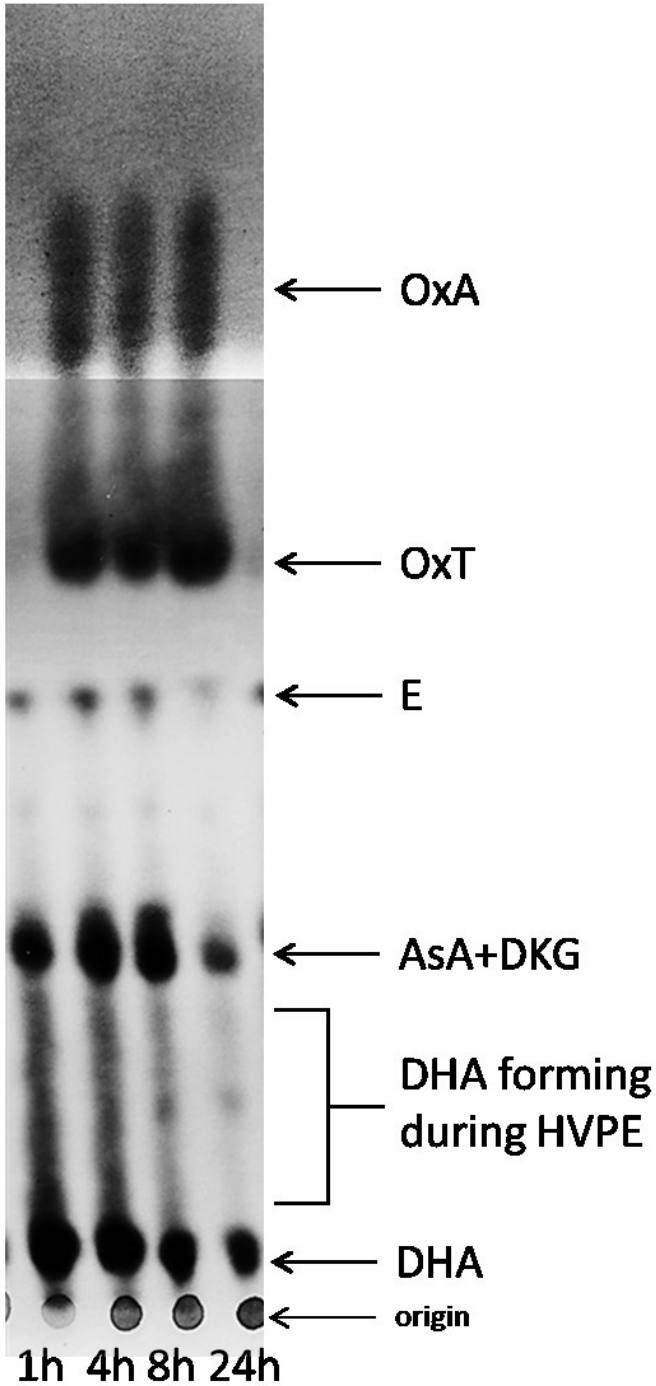
OxA
OxT
E
AsA+DKG
DHA forming during HVPE
DHA
origin
1h 4h 8h 24h

b

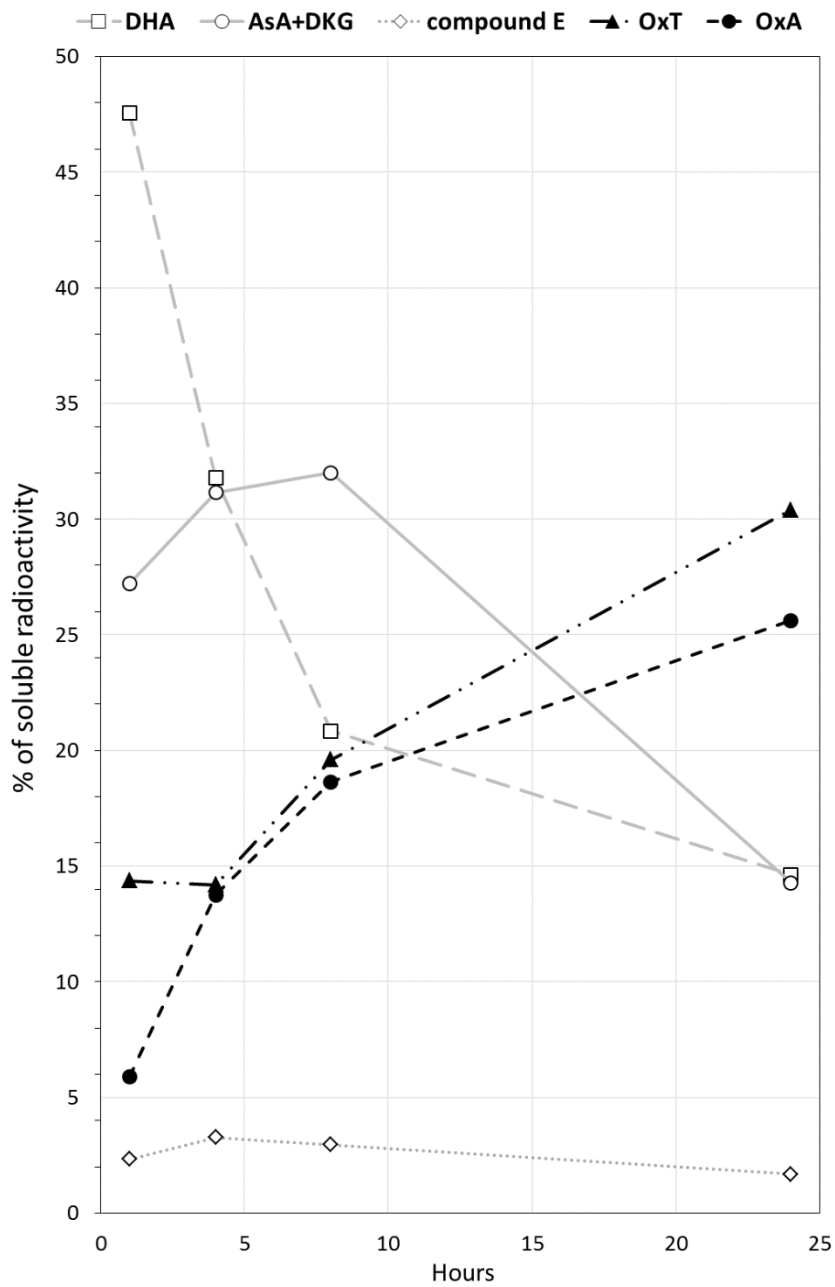
DHA
AsA+DKG
compound E
OxT
OxA
% of soluble radioactivity
Hours
0
5
10
15
20
25
30
35
40
45
50

Fig. 5

a

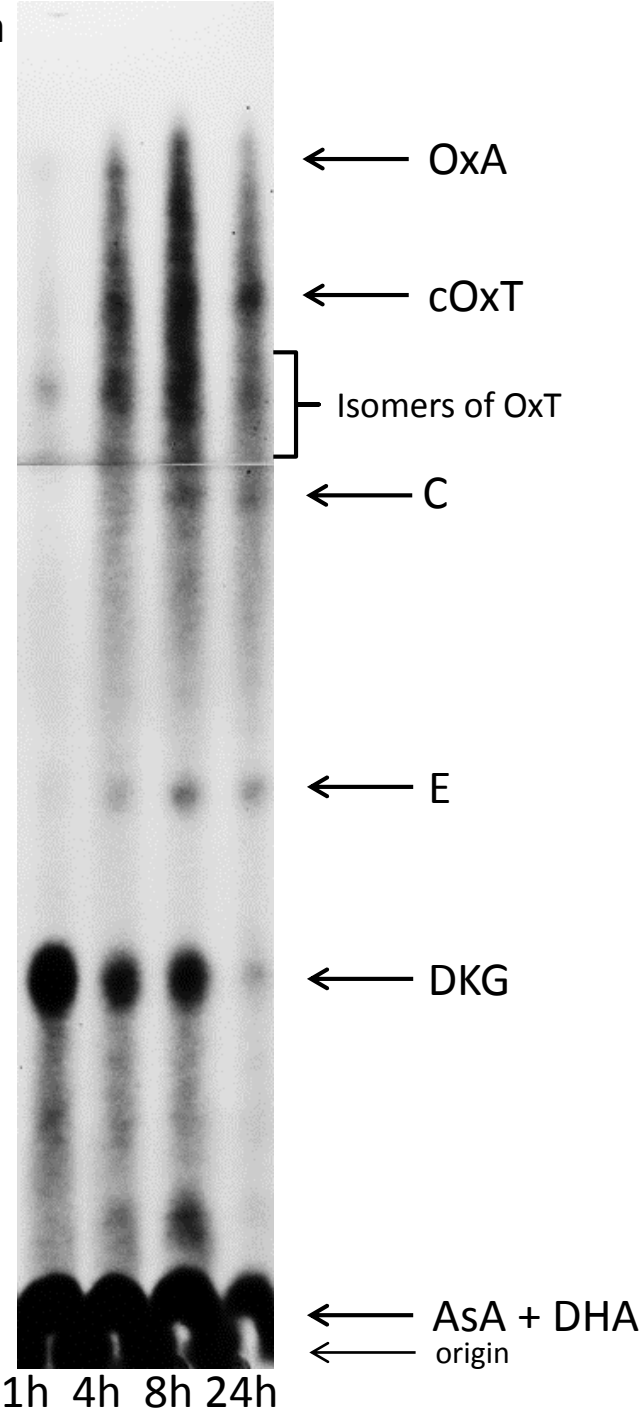
OxA
cOxT
Isomers of OxT
C
E
DKG
AsA + DHA
origin
1h 4h 8h 24h

b

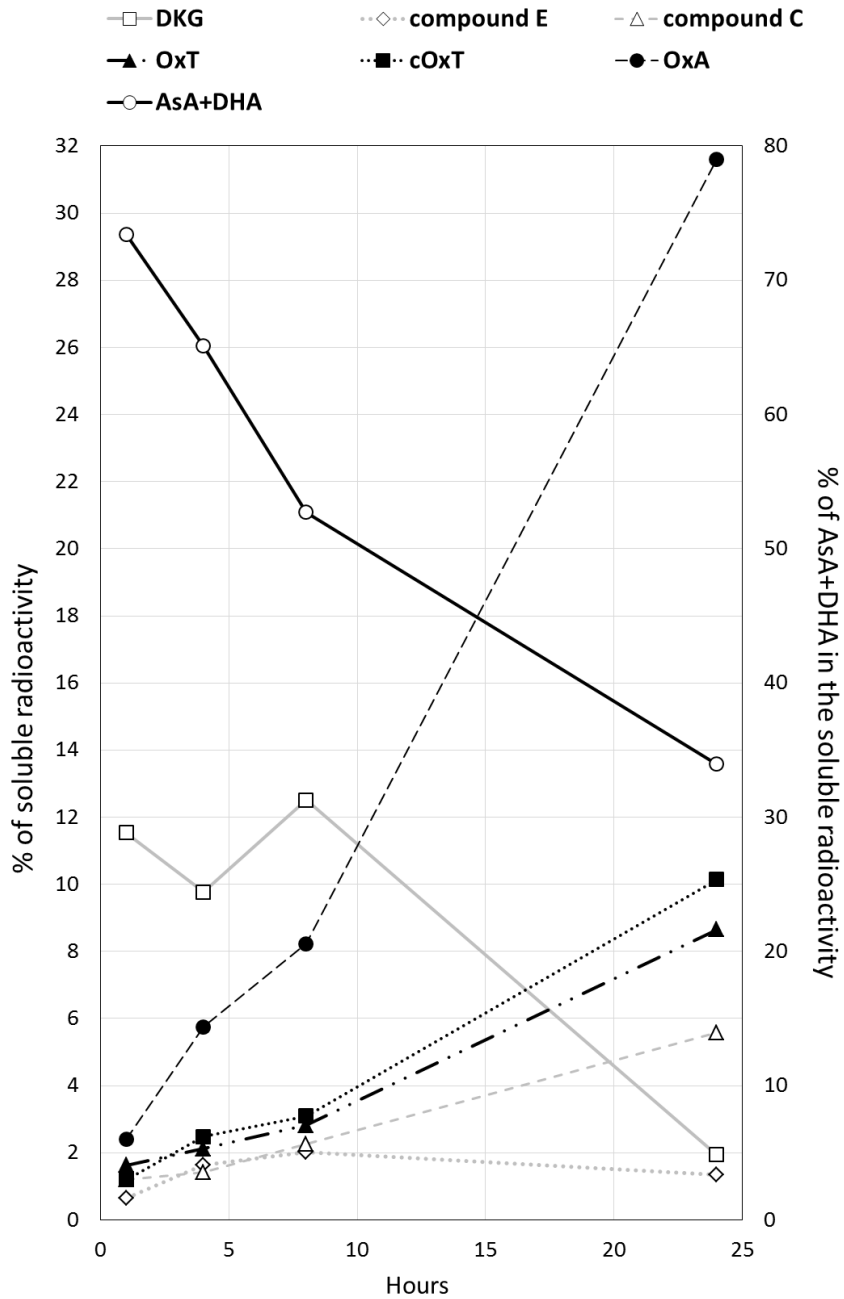
DKG
compound E
compound C
OxT
cOxT
OxA
AsA+DHA
% of soluble radioactivity
% of AsA+DHA in the soluble radioactivity
Hours
0
2
4
6
8
10
12
14
16
18
20
22
24
26
28
30
32
0
10
20
30
40
50
60
70
80
0
5
10
15
20
25

Table 2

		mg.100gFw $^{-1}$				*arbitrary unit.gFw* $^{-1}$		*arbitrary unit.gFw* $^{-1}$
	AsA	p<0.05	**DHA**	p<0.05	**OxA**	p<0.05	**ThrO**	p<0.05
high light	127.9	*a*	26.7	*a*	8.9	*c*	1.3	*b*
48h dark	33.1	*b*	8.0	*b*	48.0	*a*	16.8	*a*
low light	41.8	*b*	8.5	*b*	5.7	*c*	0.5	*b*
48h dark	9.0	*c*	3.0	*c*	30.6	*b*	2.5	*b*

Fig. 6

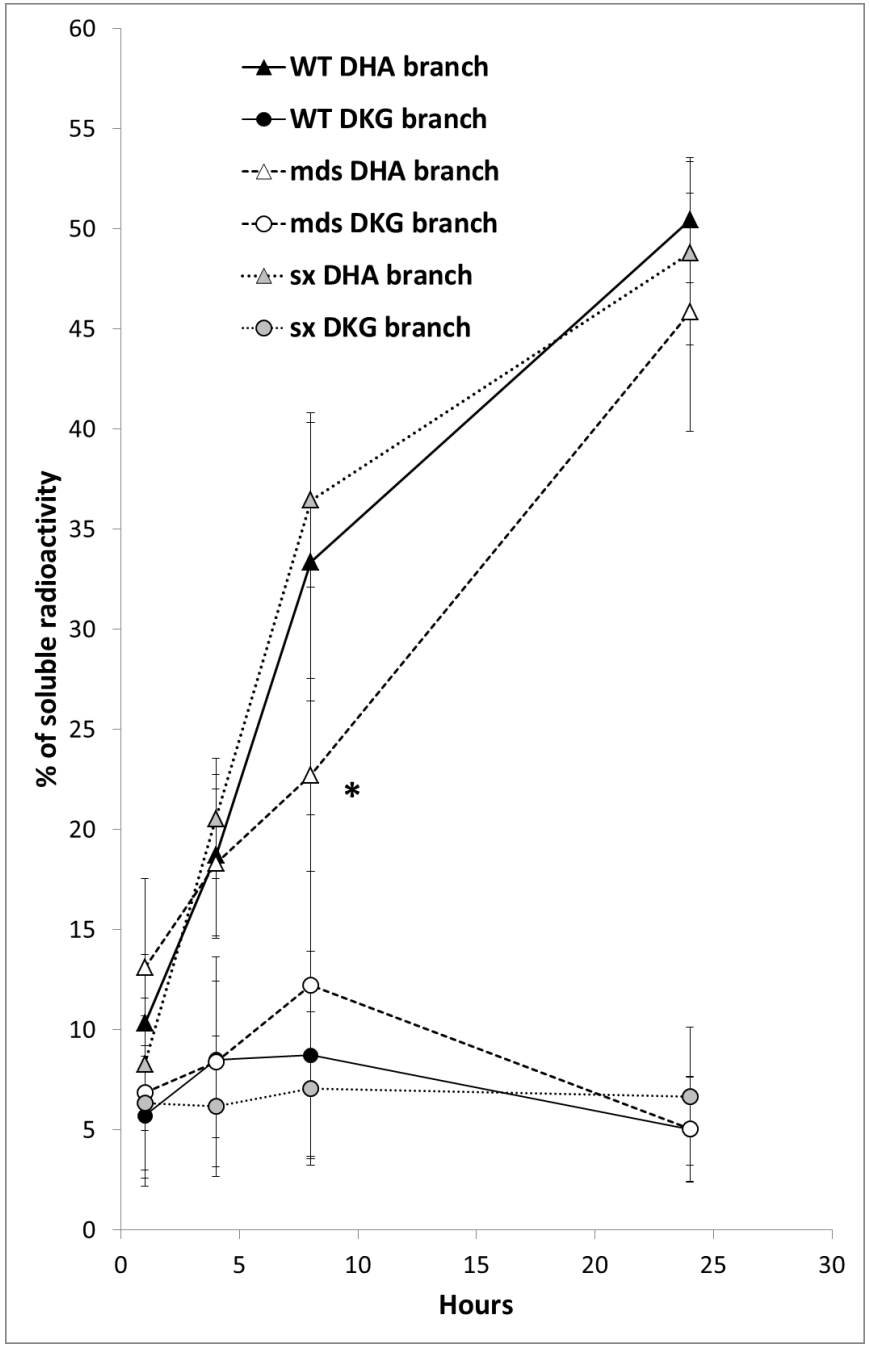
WT DHA branch
WT DKG branch
mds DHA branch
mds DKG branch
sx DHA branch
sx DKG branch
% of soluble radioactivity
Hours
*
0
5
10
15
20
25
30
35
40
45
50
55
60
0
5
10
15
20
25
30

Table 3

	% of 14C recovered in AsA+DHA after 24h	p<0.1	% of 14C recovered in degradation products after 24h	p<0.1
WT	37 ±6.2	a	63 ±9.9	a
mds42	37 ±11.7	a	63 ±18.7	a
mds5	43 ±2.8	a	57 ±2.8	a
sx1.7	30 ±3.3	a	70 ±3.3	a
sx6.10	41 ±4.2	a	59 ±1.5	a

Fig. S1

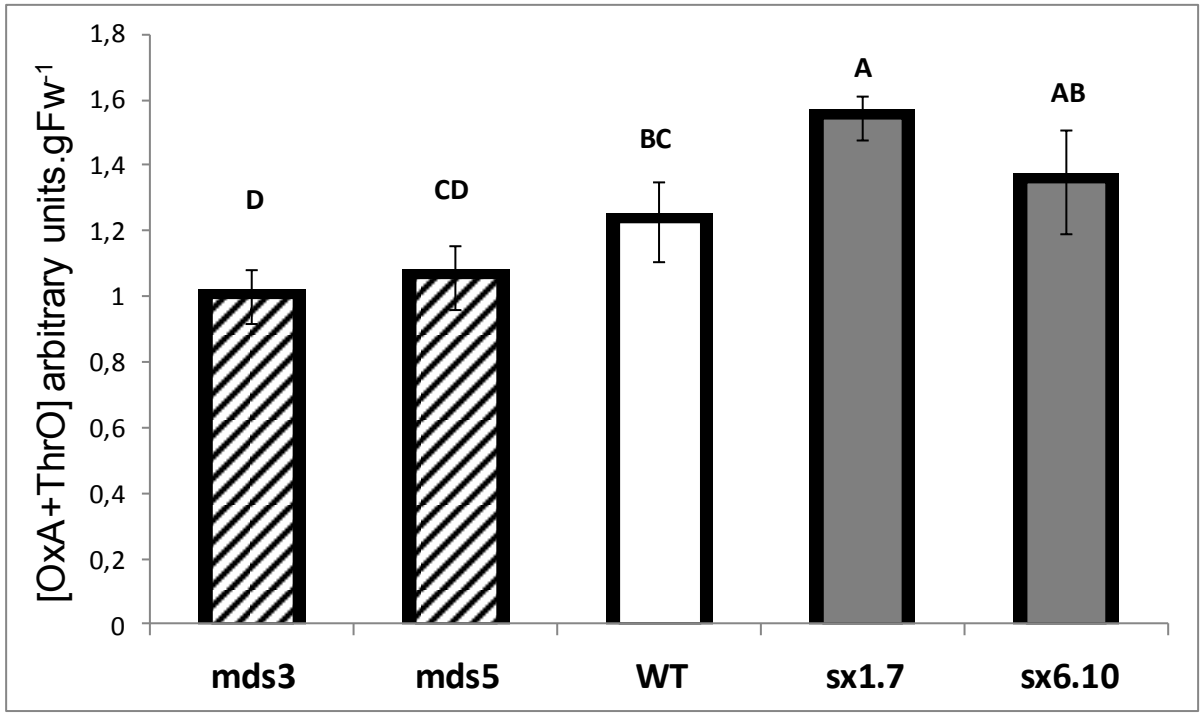
[OxA+ThrO] arbitrary units.gFw-1
1,8
1,6
1,4
1,2
1
0,8
0,6
0,4
0,2
0
D
CD
BC
A
AB
mds3
mds5
WT
sx1.7
sx6.10